Eur. Phys. J. B **21**, 547–552 (2001)

THE EUROPEAN PHYSICAL JOURNAL B

EDP Sciences

On the evolution of the ground state in the system $U_xLa_{1-x}S$: Polarized neutron diffraction and X-ray magnetic circular dichroism study

A. Bombardi[1,2,a], N. Kernavanois[1], P. Dalmas de Réotier[1], G.H. Lander[2], J.P. Sanchez[1], A. Yaouanc[1], P. Burlet[1], E. Lelièvre-Berna[3], A. Rogalev[4], O. Vogt[5], and K. Mattenberger[5]

[1] Département de Recherche Fondamentale sur la Matière Condensée, Commissariat à l'Énergie Atomique-Grenoble, 38054 Grenoble, France
[2] European Commission, Joint Research Centre, Institute for Transuranium Elements, Postfach 2340, 76125 Karlsruhe, Germany
[3] Institut Laue Langevin, 38043 Grenoble, France
[4] European Synchrotron Radiation Facility, 38043 Grenoble, France
[5] Laboratorium für Festkörperphysik, Eidgenössische Technische Hochschule-Zürich, 8093 Zürich, Switzerland

Received 31 January 2001

Abstract. In the $U_xLa_{1-x}S$ system there is an abrupt loss of the long-range ferromagnetic ordering found in pure US at a critical concentration $x_c \sim 0.57$, which is far above the percolation limit. As the magnetic ground state in such a system can be strongly affected by small variations of the $5f$ localization, we have investigated a set of samples with different x by polarized neutron diffraction and X-ray magnetic circular dichroism (XMCD). The neutron results are consistent with early measurements performed on pure US. Even at the lowest U content ($x = 0.15$, below x_c) the shape of the induced form factor ($f(Q)$) is comparable with that found for $x = 1$ and is well reproduced by either a U^{4+} or a U^{3+} state. The ratio between the orbital and the effective spin moments in the XMCD measurements confirms this result, but the evolution of the shape at the M_5 edge suggests an abrupt change in the distribution of the electrons (holes) in the $5f$ density of states around x_c.

PACS. 87.64.Ni Optical absorption, magnetic circular dichroism, and fluorescence spectroscopy – 75.25.+z Spin arrangements in magnetically ordered materials (including neutron and spin-polarized electron studies, synchrotron-source X-ray scattering, etc.)

1 Introduction

The light actinide (An = U, Np, Pu) monopnictides and monochalcogenides with the fcc NaCl-type structure are fascinating systems. Due to the extension of the An $5f$ electrons, their electronic properties strongly depend on the chemical environment. Even if the interactinide distances prevent direct overlap between the $5f$ electrons from neighbouring sites, their interactions are strongly modified *via* the hybridization with the anion p orbitals and band and valence electrons. In the ferromagnetic U monochalcogenides, both the ordered and effective magnetic moments are strongly reduced compared to that expected from free-ion calculations, and the ordering temperature T_C decreases with increasing anion radius.

One way to modify the interactions in these compounds is dilution by non-magnetic elements. In the case of the $U_xLa_{1-x}S$ system a diamagnetic non f ion is substituted for the U ions; this increases the lattice parameter and reduces the magnetic exchange. The properties of US have been studied for a long time [1]. Recently the $U_xLa_{1-x}S$ system has been studied by various techniques both experimentally [2–4] and theoretically [5]. From their transport and magnetization measurements Schoenes *et al.* [2] conclude that the $5f$ electronic localization varies non-monotonically with x. Neutron diffraction studies [3,6] on US and USe system diluted with trivalent La show that at $x_c \simeq 0.57$ and $\simeq 0.55$, respectively, there is an abrupt disappearance of the long-range magnetic ordering. In addition, the electronic contribution to the specific heat at low temperature in the US based system doubles [3] around x_c. The collapse of the ferromagnetic ordering is also predicted by Cooper *et al.* [5] who treat the problem in terms of a variation of the electronic localization. The $U_xLa_{1-x}S$ solid solution has been studied also by muon spin relaxation and rotation [4] (μ-SR) and the authors claim that there is a collapse of the magnetic moment μ around x_c (at $x = 0.4$, $\mu \approx 0.05\mu_B/U$) but that the magnetic ordering is present down to $x = 0.15$, which is close to the conventional percolation limit ($x \sim 0.14$). From

[a] e-mail: bombardi@ill.fr

the available μ-SR data, it is not possible to distinguish between short-range and long-range magnetic ordering since, compared to unpolarized neutrons, it is sensitive to very small magnetic moments, so that the two results may not contradict each other.

All authors agree that the abrupt change observed between the low U content range ($x \leq 0.55$) and the high U content range ($x \geq 0.60$) should be ascribed to a different $5f$ electron behavior in the two concentration regimes.

To directly measure the character of the $5f$ electrons we have performed two series of experiments. The first is the determination of the magnetic form factor, the Fourier transform of the magnetization distribution of unpaired electrons "localized" on a magnetic ion, by polarized neutron diffraction. The results are compared to those on pure US [7]. Within the dipolar approximation these data can be interpreted, in terms of the orbital, μ_L, and the spin, μ_S, U moments. As discussed below, these values depend somewhat on the valence state attributed to the magnetic ion, which is not firmly established in actinide metallic systems [1]. Whatever the valence, a $5f$ delocalization should be accompanied by a relative quenching of the orbital moment, in the sense that $\frac{|\mu_L|}{|\mu_S|}$ is reduced from the free-ion value, for example in UFe_2 (Refs. [8,9]), where the $5f$ electrons are almost completely delocalized, $\frac{-\mu_L}{\mu_S} \simeq 1$, whereas in US (Refs. [8,10]) $\frac{-\mu_L}{\mu_S} \simeq 2.4$.

A further set of experiments involves XMCD measurements at the U $M_{4,5}$ edges. This measurement exploits the different absorption of a material to the passage of circularly polarized light of opposite helicity in the presence of a magnetic moment. This difference, the dichroic signal, is strongly enhanced near the resonant transitions from core to valence states, in the presence of strong spin-orbit coupling. Since the $M_{4,5}$ absorption edges involve transitions $3d \rightarrow 5f$, they give access to the $5f$ density of state above the Fermi level. The sum rules for the orbital [11] and the spin [12] moments, which relate the area of the dichroic signals, respectively, to $\langle L_z \rangle (= -\mu_L/\mu_B)$ and $\langle S_e \rangle = \langle S_z \rangle + 3\langle T_z \rangle$ with $\langle S_z \rangle (= -\mu_S/2\mu_B)$, and the magnetic dipole operator $\mathbf{T} = \sum_i [\mathbf{s}_i - 3\mathbf{r}_i(\mathbf{r}_i \cdot \mathbf{s}_i)/r_i^2]$, allow for an estimation of μ_L and, if $\langle T_z \rangle$ is known, of μ_S in ferromagnets, ferrimagnets and even paramagnets in which a large moment can be induced. In some cases $\langle T_z \rangle$ can be neglected and the sum rules provide directly $\langle L_z \rangle$ and $\langle S_z \rangle$. However, this advantage is generally not present in actinide systems, which implies that we have access only to the effective spin $\langle S_e \rangle$.

The shape of the dichroic signal depends on the occupancy and the energy spread of the magnetic sublevels that comprise the investigated density of state. These features depend on the chemical environment, and may provide qualitative information on subtle electronic changes occurring in the system.

2 Experimental

All the samples were prepared at the ETH Zürich by the mineralization technique [13]. They have approximately parallelepiped shape and volumes of few cubic mm. The magnetic form factor measurements were performed with the polarized neutron diffractometer D3 installed on the hot source at the ILL. The samples were oriented with a 3-fold axis vertical (which is the easy-axis for ordered materials) in a cryomagnet and field cooled in the maximum available field of 6 T down to 2 K. According to the hysteresis loop, this saturates the magnetic moment and produces monodomain samples. The intensity ratios (the so-called flipping ratios) of the Bragg peaks were measured with neutrons polarized first parallel and then antiparallel to the applied field. Flipping ratios were collected with a neutron wavelength $\lambda = 0.843$ Å, and to control the extinction correction some reflections were measured also at $\lambda = 0.514$ Å. Extinction was quite small in the samples examined ($x = 0.60$, 0.40, and 0.15), and this is consistent with the results of the previous unpolarised neutron diffraction experiment [3]. Data were also corrected for the $\lambda/2$ contamination and the incomplete polarization of the neutron beam.

XMCD measurements were performed at the beamline ID12A at the ESRF by sweeping the energy of the X-ray beam across the M_4 ($\sim$ 3726 eV) and M_5 ($\sim$ 3551 eV) U absorption edges. As the crystals were too thick to directly measure the absorption and we were interested in the bulk properties, we monitored the fluorescence yield of the relaxation process. The resulting signal comes from the first $\sim$ 3000 Å of the samples ($\approx$ 500 cells). It was not possible to have exactly the same experimental conditions as in the neutron experiments. In the dichroism case the crystals ($x = 0.60$, 0.40, and 0.30) were oriented with a 4-fold axis forming an angle of $\sim 10°$ with the X-ray beam. The samples were cooled in a magnetic field parallel to the incident beam. The two absorption spectra needed to extract the dichroic signal were obtained by flipping the direction of the applied magnetic field. To avoid the crystal breaking, due to the large anisotropy present at low temperature for $x \geq x_c$, the $x = 0.60$ sample was cooled only to 90 K in a 2 T field, whereas for $x = 0.40$ and 0.30 the applied field was 5 T and the temperature $T \sim 10$ K.

Magnetization measurements were performed with a SQUID magnetometer in the same orientations and with the same applied fields as the neutron and dichroism measurements in order to allow a comparison. All the results presented in this report are normalized to saturation.

3 Magnetic form factor

The measured form factor $f(Q)$, times the magnetic moment per U ion measured with neutron μ_{neu}, for both $x = 0.60$ and $x = 0.40$ samples are reported in Figure 1a. For comparison the results for pure US are also shown in Figure 1b. The values for the scattering vector $Q = 0$ are taken from magnetization measurements. At moderately low Q values ($Q \leq 0.6$ Å^{-1}), using the Johnston approach [14], $\mu_{neu} f(Q) \simeq \mu_{neu}(\langle j_0 \rangle + C_2 \langle j_2 \rangle)$, where the $\langle j_i \rangle$ are the spherical Bessel function transform of the radial part of the $5f$ single electron wavefunction, and $C_2 = \mu_L/\mu_{neu}$. At larger Q values, the higher order terms

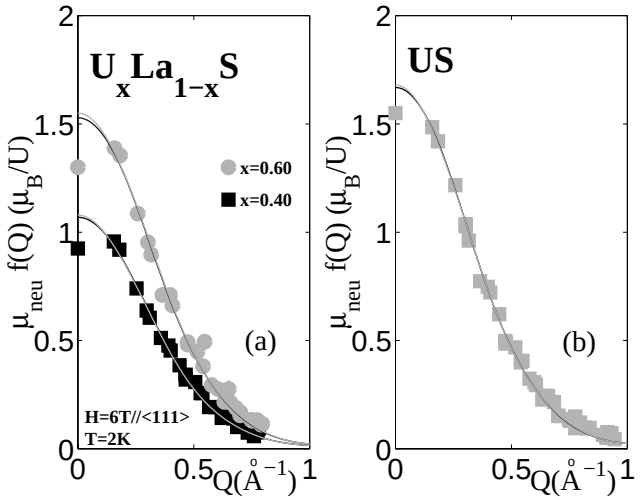

Fig. 1. (a) the present measurements at $x = 0.40$ and $x = 0.60$. (b) the magnetic form factor of pure US [7]. For each sample there are two solid lines, almost indistinguishable, corresponding to the fits with the hypotheses f^3 and f^2 states. The points at $Q = 0$ are obtained by magnetization measurements.

Table 1. Parameters obtained by the dipolar fit to the neutron data with the U^{3+} hypothesis. The data for pure US are obtained from a new fit of the Wedgwood data [7]. $\overline{\mu}$ is obtained by the magnetization measurements and is reported for comparison. The magnetic moments are given in μ_B/U. The double vertical line divides the samples exhibiting long range magnetic ordering (LRMO) from the others (NO LRMO). The value for $-\mu_L/\mu_S$ for a free-ion U^{3+} state including intermediate coupling is 2.55.

	NO LRMO		LRMO	
U^{3+}	$x = 0.15$	$x = 0.40$	$x = 0.60$	$x = 1$ [7]
$T(K)$	2	2	2	4.2
$\mu_{neu} = \mu_L + \mu_S$	0.11(1)	1.07(2)	1.53(6)	1.67(3)
$C_2 = \frac{\mu_L}{\mu_{neu}}$	2.0(1)	1.76(6)	1.9(1)	1.86(6)
μ_L	0.22(2)	1.88(7)	2.9(3)	3.11(11)
$-\mu_S$	0.110(14)	0.81(7)	1.38(16)	1.4(1)
$-\frac{\mu_L}{\mu_S}$	2.0(1)	2.32(10)	2.11(12)	2.16(8)
$\overline{\mu}$	0.097(3)	0.925(2)	1.30(3)	1.55 [2]

start to be important. Only flipping ratios corresponding to $Q \leq 0.6$ Å^{-1} were considered. The data were fitted assuming two hypotheses for the U ground state (U^{3+} and U^{4+}). At each x, both the ionic states fit well the experimental results, so, as in the case for pure US, it is not possible to establish which is the actual ground state. The resulting parameters for the 3+ and 4+ configurations are reported in Table 1 and Table 2 respectively. The saturated magnetic moment per U increases with increasing x, but the ratio μ_L/μ_S is constant within the experimental sensitivity. The two fits give slightly different values of the ratio μ_L/μ_S for the different configurations because of the different spatial extent of the $\langle j_i \rangle$ functions [15]. The

Table 2. Same captions as in Table 1, but with the hypothesis of U^{4+} ionic configuration. The value for $-\mu_L/\mu_S$ for a free-ion U^{4+} state including intermediate coupling is 3.34.

	NO LRMO		LRMO	
U^{4+}	$x = 0.15$	$x = 0.4$	$x = 0.6$	$x = 1$ [7]
$T(K)$	2	2	2	4.2
$\mu_{neu} = \mu_L + \mu_S$	0.114(12)	1.079(13)	1.55(6)	1.68(3)
$C_2 = \frac{\mu_L}{\mu_{neu}}$	1.67(12)	1.58(5)	1.71(11)	1.67(5)
μ_L	0.19(2)	1.70(5)	2.6(2)	2.81(6)
$-\mu_S$	0.076(16)	0.62(4)	1.10(18)	1.13(9)
$-\frac{\mu_L}{\mu_S}$	2.5(3)	2.74(14)	2.4(2)	2.49(11)

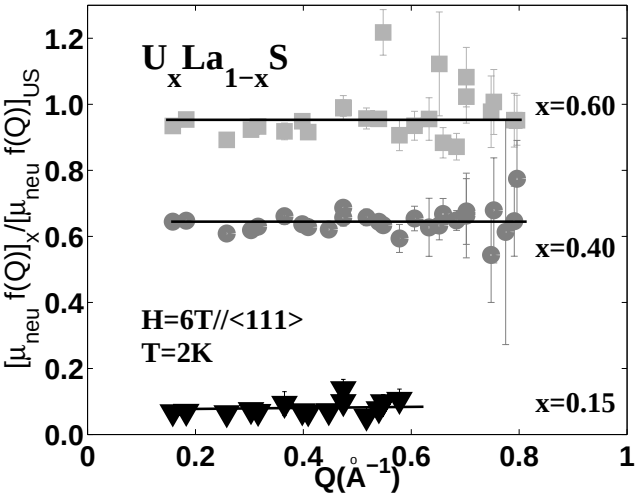

Fig. 2. Ratio between the form factors obtained by the present experiment at $x = 0.60$, 0.40 and 0.15 and that given in reference [7] as function of Q.

bulk magnetization measurements values at $x = 0.60$ and $x = 0.40$ were found to be reduced by about ($\sim 0.15\,\mu_B$) compared with the neutron results and the same difference was measured also in pure US. This difference has been attributed to the conduction electrons ($6d$ and $7s$) which have a spatial extent such that they cannot be observed by neutron experiments [15]. In agreement with theory [23], these electrons are polarized parallel to the uranium spins and thus antiparallel to the total U moment.

According to Figure 1, we conclude that the shape of the form factor does not change when varying the U concentration. This is further demonstrated in Figure 2, where we plot the ratio between the form factors measured in dilute compounds and the form factor measured in pure US as a function of Q. The magnetization distribution in real space, obtained by the maximum entropy technique [16], agrees with the hypothesis of the magnetic moment only at the U sites.

4 Dichroism results

In this section we focus on two aspects: a quantitative analysis of the dichroic data and a qualitative comparison of the shapes of the dichroic signals that change abruptly near x_c.

The quantitative analysis of dichroism results on thick samples follows a well-established procedure [17]. The sum rules have been established for absorption in ideal conditions (*e.g.* beam perfectly polarized, absence of background), but they still hold in fluorescence mode [18,19].

Recently, the intrinsic approximation included in the sum rules has been directly checked, performing dichroism measurements in *absorption* at the $L_{2,3}$ edges of Fe and Co thin layers. Chen *et al.* [20] estimated the probable error as 7% for the individual $\langle L_z\rangle$ and $\langle S_z\rangle$ values ($\langle T_z\rangle$ being negligible in these materials) and as 3% for the ratio $\frac{\langle L_z\rangle}{\langle S_z\rangle}$, where, due to the simultaneous use of the two sum rules, there is no need to estimate the area of the absorption white lines. The situation should be even better at the U $M_{4,5}$ edges. In fact, a possible source of error at the $L_{2,3}$ edges in the Fe and Co systems is the small spin-orbit coupling that makes it difficult to separate well in energy the two edges ($\Delta E \approx 10$ eV), whereas the M_4 and M_5 edges in actinides, due to the large spin orbit coupling of the core $3d$ states, are well separated in energy ($\Delta E \approx 175$ eV).

In our case, however, the data analysis requires obtaining the absorption from the fluorescence signal, and the need to correct for the self-absorption in the material [21]. The data treatment introduces systematic errors that must be estimated. A detailed description of the procedure adopted and a careful analysis of the effect of the variation of the parameters involved in the treatment is given in reference [22].

The absorption and the dichroic spectra, corresponding to the $M_5(3d_{5/2} \rightarrow 5f)$ and M_4 $(3d_{3/2} \rightarrow 5f)$ edges are shown in Figure 3 for the studied concentrations and for pure US. The M_4 spectra are featureless and their shapes do not change with x. As usual in uranium compounds the ratio of the dichroic amplitudes M_4/M_5 is ~ 5. The M_5 edge at $x = 0.60$ is very similar to that measured in pure US [10,22], with a negative lobe and a small positive "splinter". At $x = 0.40$ and 0.30 the M_5 edges exhibit two lobes that have almost equivalent areas.

Excluding uncertainties arising from the application of the sum rules, $\langle L_z\rangle/3n_h$, where n_h is the number of the holes in the $5f$ shell, has a possible error of $\sim 7\%$ whereas $\frac{\langle L_z\rangle}{\langle S_e\rangle}$ error is $\sim 1\%$. This, combined with experimental errors, allows to set an upper bound for the global uncertainties of $\sim 10\%$ on $\langle L_z\rangle/3n_h$ and of $\sim 4\%$ on $\frac{\langle L_z\rangle}{\langle S_e\rangle}$.

The results are reported in Table 3 for the two hypotheses $3+$ ($n_h = 11$) and $4+$ ($n_h = 12$) for the U valence state. To allow a comparison with the neutron results, the dichroism results have been normalized, using magnetization measurements, to conditions of field and temperature corresponding to the neutron experiments. The ratio $\frac{\langle L_z\rangle}{\langle S_e\rangle}$ appears to be lower for the low x sample, but, within our statistics, we cannot claim a change of this parameter as a function of x. This result implies that no abrupt variation of the electronic localization occurs across the series. To estimate $\langle S_z\rangle$, $\langle T_z\rangle$ and the total $5f$ moment μ_{dic}, we use the ratio $\frac{\mu_L}{\mu_S}$ obtained by the fits of the magnetic form factors.

Table 3. Parameters obtained by the dichroism experiments with the two hypotheses $n_h = 11$ (U^{3+}) and $n_h = 12$ (U^{4+}). The results obtained by magnetization measurements have been used to deduce the expected values in the same conditions of the magnetic form factor measurements. The ratio $-\frac{\langle L_z\rangle}{\langle S_e\rangle}$ and R are not affected by the hypothesis on hole number. The double vertical line divides the samples exhibiting long range magnetic ordering (LRMO) from the others (NO LRMO).

	NO LRMO		LRMO	
$U^{3+}(n_h = 11)$	$x = 0.30$	$x = 0.40$	$x = 0.60$	$x = 1$ [22]
$-\langle L_z\rangle$	1.0(2)	1.4(2)	2.3(4)	2.6(4)
$\langle S_e\rangle$	0.7(1)	1.0(2)	1.3(3)	1.7(4)
$\langle T_z\rangle$		0.29(3)	0.33(3)	0.39(3)
$\mu_{dic}(\mu_B/U)$		0.8(1)	1.2(2)	1.4(3)
$U^{4+}(n_h = 12)$	$x = 0.30$	$x = 0.40$	$x = 0.60$	$x = 1$ [22]
$-\langle L_z\rangle$	1.1(2)	1.5(3)	2.5(5)	2.9(5)
$\langle S_e\rangle$	0.76(15)	1.1(2)	1.4(3)	1.9(5)
$\langle T_z\rangle$		0.28(3)	0.32(3)	0.38(3)
$\mu_{dic}(\mu_B/U)$		0.95(14)	1.5(3)	1.7(3)
$-\frac{\langle L_z\rangle}{\langle S_e\rangle}$	1.43(7)	1.44(7)	1.73(8)	1.56(6)
$R = \left\lvert\frac{A}{B}\right\rvert$	2.1(6)	2.4(7)	16(2)	23(3)

5 Discussion

The polarised neutron study has confirmed the previous results on US. Although the long range order is lost at $x_c = 0.57$ (Ref. [3]), no change appears in the shape of the magnetic form factor either near x_c, or at lower x when the induced moment is quite small. Within the dipole approximation, this implies that the ratio of μ_L/μ_S is unchanged as a function of x. Averaging the experimental values given in Tables 1 and 2, we find $|\mu_L/\mu_S| = 2.5(1)$ for the assumption of $U^{4+}(5f^2)$, and about 2.1(1) for $U^{3+}(5f^3)$, whereas the calculated free-ion values for these two configurations, using intermediate coupling, are 3.34 and 2.55. *Ab initio* study of US have suggested that there are about 2.9 $5f$ electron states occupied [23], so that US should be closer to the U^{3+} configuration.

The decrease in $|\mu_L/\mu_S|$ from the free ion value of 2.55 to 2.1(1) is due to hybridization. However, this aspect of the hybridization does not change with La dilution, suggesting it is a single-ion effect, presumably involving the $5f$ and conduction electrons $6d7s$ at the U site.

Another comparison may be made between the polarised neutron results and XMCD by examining the

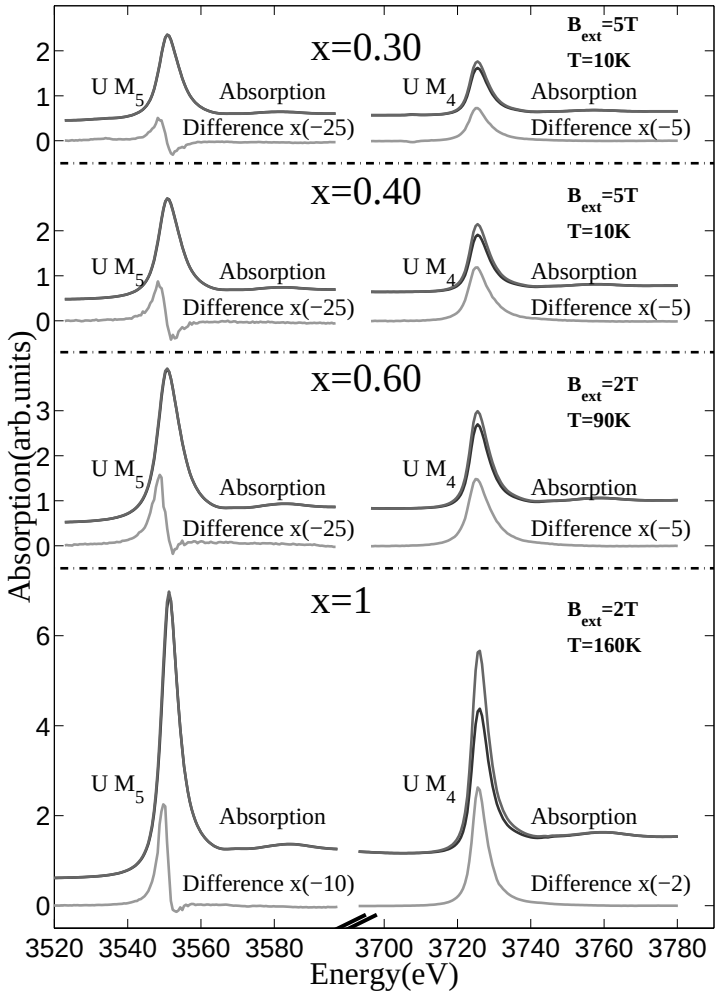

Fig. 3. $M_{4,5}$ absorption spectra and corresponding dichroism spectra (light gray) at $x = 0.30$, 0.40, 0.60, and 1. The value of the applied magnetic field ($B_{\rm ext}$) and the temperature (T) are reported on the right for each sample. At $x = 0.30$ and 0.40 the areas of the positive and the negative lobes at the M_5 absorption yields are comparable. On a further increase of x ($x \geq 0.60$) the positive lobe becomes much larger than the negative one, which is reduced to a small "splinter".

orbital moment μ_L and $-\langle L_z\rangle$ in the three tables. Here the agreement is reasonable with the assumption of U^{4+}, whereas in the case of U^{3+} the dichroism values are consistently $\sim 0.5\mu_{\rm B}$ smaller than those deduced from neutron. This suggests a U^{4+} ground state, in contradiction with theory. Of course, we must be aware that both the neutron and XMCD results have been deduced using free atom parameters. In the neutron case by applying the dipole approximation [14], about which there has recently been some doubt expressed [25], and by using atomic $\langle j_i\rangle$ functions [15]. In the dichroism case, using sum rules based on atomic states [11,12] and completely neglecting coherence effects, could modify the ratio between the dichroic signals [26]. The lack of agreement is therefore not totally surprising, and illustrates the difficulty of establishing the valence state of U in these materials, as discussed earlier.

From the dichroism alone we see that the ratio $-\langle L_z\rangle/\langle S_{\rm e}\rangle$ shows a slight increase for $x > 0.50$, but this is barely significant within the statistics. Moreover, $\langle T_z\rangle$ is close to the latest *ab initio* value of 0.27 of this quantity [24], as well as the 0.36 deduced by Shishidou *et al.* [27] There seems to be a slight tendency for $\langle T_z\rangle$ to rise with x, as perhaps might be expected since $\langle T_z\rangle$ is also a measure of anisotropy, and US is known to be highly anisotropic [1].

In order to obtain the mean value of the magnetic moments, and the parameters that appears in Table 3, the average value over the magnetic sublevels, spin down and spin up, is taken. There does not seem to be a major change in the electronic structure in the *integrated* properties of the $U_xLa_{1-x}S$ system as a function of x, apart, of course, from the loss of the long-range ordered moment for $x < x_{\rm c}$, as shown in reference [3]. On the other hand, it is also clear from the muon experiment, as well as our own neutron inelastic scattering measurements [28], that even for $x \leq 0.40$ ordered magnetic moments exist and exhibit short-range ferromagnetic correlations. This is not a situation in which the local moment cease to exist below $x_{\rm c}$.

One property that does change drastically as a function of x is the spectral shape of the M_5 dichroic signal – see Figure 3. This change can be emphasized by examining

the areas of the positive and negative lobes at the M_5 edges for all the materials shown in Figure 3. We have attempted to be more quantitative in this respect by summing the experimental points corresponding to the individual positive and negative lobes around the M_5 dichroic signal, and taking their ratio. This is shown in Table 3 as $R = |A/B|$, where A is the area of the lobe at lower energy (negative with our sign convention), and B the area of the lobe at higher energy (positive with our convention). The dispersive nature of the line shape may be seen clearly for the low x concentrations, where $R \sim 2$, whereas for $x = 0.60$ and 1, $R > 10$. Note that this feature of the dichroic signal will not appear in any *integrated* property of the dichroism, as the total area under the dichroic curve is taken, independent of sign, in deducing the parameters in Table 3.

This negative "splinter", as it was called by Shishidou *et al.* [27], has been discussed by these authors and by Dalmas de Réotier *et al.* [29]. There is agreement where this effect comes from qualitatively; it is related to the energy splitting and to the change in the population of the $|JJ_z\rangle = |7/2\ \pm m_{7/2}\rangle$ states, see Figure 4b of reference [27], and leads to unequal energy dependencies of the two transitions. It is not seen at the M_4 edge because there are no dipolar matrix elements to the unoccupied $|7/2\ m_z\rangle$ states from the $3d_{3/2}$ core state, which is relevant to the M_4 edge.

However, such a model in jj coupling is too naive to be more than qualitatively satisfactory, and requires more complete calculations to simulate the experiments. A simple approach might assume that the splitting is proportional to the molecular field at the U site, and hence the magnetic moment, either ordered or induced by a magnetic field. If this was the case one would expect the biggest change in R to come at low x, where the observed moment drops appreciably. However, this is not the case, the biggest change is near x_c, so that one may perhaps associate this change also with the loss of the long range magnetic order. In conclusion on this point we note that there is little consistency of the spectral features of the M_5 dichroic signal for U compounds. R is large in US and URu_2Si_2, it is small in the low x compositions examined here, smaller in UPt_3, and UPd_2Al_3, and even less than one in UBe_{13} [29]. Hopefully, a theoretical treatment can shed some light on this unusual systematics.

Further experiments, such as photoemission to examine the electronic structure, and EXAFS to examine the nature of the atomic disorder near x_c are in progress.

A.B. acknowledges the European Commission for support given in the frame of the programme "Training and Mobility of the Researchers".

References

1. *Handbook on the Physics and Chemistry of the Actinides*, edited by A.J. Freeman, G.H. Lander (Elsevier Science, Amsterdam) Vols. 1 (1984) and 2 (1985).
2. J. Schoenes, O. Vogt, J. Loehle, F. Hulliger, K. Mattenberger, Phys. Rev. B **53**, 14987 (1996).
3. F. Bourdarot, A. Bombardi, P. Burlet, R. Calemczuk, G.H. Lander, F. Lapierre, J.P. Sanchez, K. Mattenberger, O. Vogt, Eur. Phys. J. B **9**, 605 (1999).
4. G. Grosse, G.M. Kalvius, A. Kratzer, E. Schreier, F.J. Burghart, K. Mattenberger, O. Vogt, J. Magn. Magn. Mater. **205**, 79 (1999).
5. B.R. Cooper, Y.L. Lin, J. Appl. Phys. **83**, 6432 (1998).
6. A. Bombardi (unpublished).
7. F.A. Wedgwood, J. Phys. C **5**, 2427 (1972).
8. G.H. Lander, M.S.S. Brooks, B. Johansson, Phys. Rev. B **43**, 13672 (1991) and references therein.
9. M. Finazzi, Ph. Sainctavit, A.M. Dias, J.P. Kappler, G. Krill, J.P. Sanchez, P. Dalmas de Réotier, A. Yaouanc, A. Rogalev, J. Goulon, Phys. Rev. B **55**, 3010 (1997).
10. S.P. Collins, D. Laundy, C.C. Tang, G. van der Laan, J. Phys. Cond. Matt. **7**, 9325 (1995).
11. B.T. Thole, P. Carra, F. Sette, G. van der Laan, Phys. Rev. Lett. **68**, 1943 (1992).
12. P. Carra, B.T. Thole, M. Altarelli, X. Wang, Phys. Rev. Lett. **70**, 694 (1993).
13. O.Vogt, in *Actinides in Perspectives*, edited by N.M. Edelstein (Pergamon, Oxford, 1982); J.C. Spirlet, O. Vogt, *Handbook on the Physics and Chemistry of the Actinides*, edited by A.J. Freeman, G.H. Lander (North Holland, 1984), Vol. 1.
14. D.F. Johnston, Proc. Phys. Soc. **88**, 37 (1966).
15. A.J. Freeman, J.P. Desclaux, G.H. Lander, J. Faber, Phys. Rev. B **13**, 1168 (1976).
16. R. Papoular, B. Gillon, Europhys. Lett. **13**, 429 (1990).
17. P. Dalmas de Réotier, J.P. Sanchez, A. Yaouanc, M. Finazzi, Ph. Sainctavit, G. Krill, J.P. Kappler, J. Goulon, C. Goulon-Ginet, A. Rogalev, O. Vogt, J. Phys. Cond. Matt. **9**, 3291 (1997).
18. M. van Veenendaal, J.B. Goedkoop, B.T. Thole, Phys. Rev. Lett. **77**, 1508 (1996).
19. S.W. Lovesey, U. Staub, J. Phys. Cond. Matt. **9**, 4271 (1997).
20. C.T. Chen, Y.U. Idzerda, H.-J. Lin, N.V. Smith, G. Meigs, E. Chaban, G.H. Ho, E. Pellegrin, F. Sette, Phys. Rev. Lett. **75**, 152 (1995).
21. C.J. Sparks, in *Synchrotron Radiation Research*, edited by H. Winick, S. Doniach (New York, Plenum, 1980), p. 459.
22. N. Kernavanois, P. Dalmas de Réotier, J.P. Sanchez, A. Yaouanc, V.Honkimäki, T. Tschentscher, J. McCarthy, A. Rogalev, O. Vogt, submitted to J. Phys. Cond. Matt.
23. M.S.S. Brooks, B. Johansson, H.L. Skriver, in *Handbook on the Physics and Chemistry of the Actinides*, edited by A.J. Freeman, G.H. Lander (Elsevier Science, Amsterdam, 1984), Vol. 1, p. 153.
24. M.S.S. Brooks (private communication).
25. K. Ayuel, P.F. de Châtel, Phys. Rev. B **61**, 15213 (2000).
26. J. Unter Dunn, D. Arvanitis, R. Carr, N. Martensson, Phys. Rev. Lett. **84**, 1031 (2000).
27. T. Shishidou, T. Oguchi, T. Jo, Phys. Rev. B **59**, 6813 (1999).
28. A. Bombardi, B. Grenier, P. Burlet, G.H. Lander, L.-P. Regnault, K. Mattenberger, O. Vogt, Physica B **276-278**, 606-607 (2000).
29. P. Dalmas de Réotier, A. Yaouanc, G. van der Laan, N. Kernavanois, J.P. Sanchez, J.L. Smith, A. Hiess, A. Huxley, A. Rogalev, Phys. Rev. B **60**, 10606 (1999).